

# Stability of Single- and Few-Molecule Junctions of Conjugated Diamines

M. Teresa González,<sup>\*,†</sup> Adrián Díaz,<sup>‡</sup> Edmund Leary,<sup>†,‡</sup> Raúl García,<sup>§</sup> M. Ángeles Herranz,<sup>§</sup> Gabino Rubio-Bollinger,<sup>‡</sup> Nazario Martín,<sup>†,§</sup> and Nicolás Agrait<sup>†,‡,||</sup>

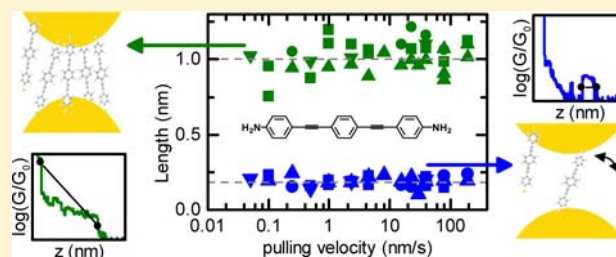
<sup>†</sup>Instituto Madrileño de Estudios Avanzados en Nanociencia (IMDEA-Nanociencia), Ciudad Universitaria de Cantoblanco, E-28049 Madrid, Spain

<sup>‡</sup>Departamento de Física de la Materia Condensada and <sup>||</sup>Instituto “Nicolás Cabrera”, Universidad Autónoma de Madrid, E-28049 Madrid, Spain

<sup>§</sup>Departamento de Química Orgánica, Universidad Complutense de Madrid, 28040 Madrid, Spain

## S Supporting Information

**ABSTRACT:** We study the stability of molecular junctions based on an oligo(phenyleneethynylene) (OPE) diamine using a scanning tunneling microscope at room temperature. In our analysis, we were able to differentiate between junctions most probably formed by either one or several molecules. Varying the stretching rate of the junctions between 0.1 and 100 nm/s, we observe practically no variation of the length over which both kinds of junction can be stretched before rupture. This is in contrast with previously reported results for similar compounds. Our results suggest that, over the studied speed range, the junction breakage is caused purely by the growth of the gap between the gold electrodes and the elastic limit of the amine–gold bond. On the other hand, without stretching, junctions would survive for periods of time longer than our maximum measurement time (at least 10 s for multiple-molecule junctions) and can be considered, hence, very stable.



## INTRODUCTION

Over recent years, the realization of molecular junctions in which only one or a few molecules are connected between two metallic electrodes has opened the possibility of directly investigating electrical transport of compounds at the ultimate level, that of a single molecule. The use of the break-junction technique as implemented by Tao et al<sup>1</sup> is, to this date, the most widely used procedure to form molecular junctions.<sup>2–7</sup> With this technique, the number and detailed positioning of molecules ultimately wired remains difficult to control precisely, however it is easy to implement, and allows the creation of hundreds and even thousands of molecular junctions readily. A rigorous statistical analysis of this large sampling of events provides consistent information about different properties of the molecular junctions, such as conductance,<sup>2,8–11</sup> thermopower,<sup>12,13</sup> or switching capability,<sup>4,14</sup> even at room temperature.

In addition, we find in the literature several attempts of exploring in more detail the processes of formation and breakage of these molecular junctions. The measurement of the force needed to break molecular junctions allows the determination of the binding strength of the molecule to the electrodes.<sup>15–17</sup> The study of the maximum elongation that a molecular junction stands before breaking provides information about the interplay between the metallic electrodes and the individual molecules which self-assemble between them.<sup>18–20</sup>

Also, by changing the speed at which a molecular junction is stretched, the stability and breaking mechanism of molecular junctions can be explored.<sup>21–24</sup> In particular, published results suggest that the junction elongation before breakage would be drastically reduced if the junctions are stretched slowly enough, indicating that the self-breaking regime of the junctions is reached. This decrease of the molecular signature in the experiments can be crucial when comparing results obtained in different experimental implementations. This is an important consideration for the field of molecular electronics, in which reproducibility of results from different laboratories has not always been obvious.<sup>25–27</sup> In addition, to know for how long an individual molecular junction can be held is vital for any possible practical application of molecular junctions between metallic surfaces.

In this paper we study the stability of molecular junctions based on an oligo(phenyleneethynylene) (OPE) diamine. Using a scanning tunneling microscope (STM), we perform break-junction experiments under ambient conditions, varying the stretching rate over more than 3 orders of magnitude. In the studied range, we observe practically no variation of the stretching elongation before rupture for the molecular junctions, suggesting that the junction breakage in these

Received: December 19, 2012

Published: March 8, 2013

experiments is caused by the pulling, with very little effect from thermal fluctuations. For this compound, we were able to differentiate between junctions which are most probably formed by one molecule from those with probably several molecules. The elongation of single-molecule junctions agrees well with the elastic stretching limit predicted theoretically for amine–gold bonds,<sup>15,28,29</sup> and it is lower than molecular length. On the other hand, for multiple-molecule junctions the elongation is around 5 times larger and agrees with a gap size between the electrodes equivalent to the molecule length, which suggests that along the stretching some individual molecules must detach and others attach. These multiple-molecule junctions were observed to survive up to 10 s in the explored range of stretching speeds.

## EXPERIMENTAL SECTION

In a break-junction experiment,<sup>30</sup> a gold wire with a nanometric neck is stretched until breakage. Along the process, the conductance of the wire,  $G$ , equals essentially that of the breaking neck, which is significantly more resistive than the rest of the wire. Its variation is recorded during the stretching along the wire axis direction,  $z$ , to generate  $G$  vs  $z$  traces. When the stretching experiment is done in the presence of molecules which self-assemble on gold, after the gold-contact breakage, a molecular junction can form if one molecule (or a few) extends across the ends of the gold wire. The molecular junction is then the most resistive part of the circuit.

Along a  $G$  vs  $z$  curve, the regions of approximately constant  $G$  (plateaus) indicate that the gold contacts or molecular junctions remain relatively unaltered during the stretching, while the regions for which there are jumps in conductance indicate structural changes. Figure 1 shows examples of these  $G$  vs  $z$  traces measured in the

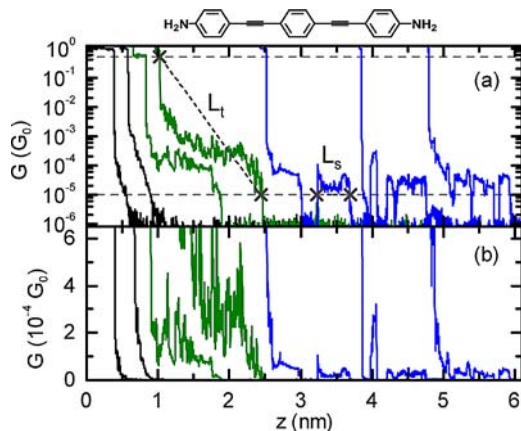


**Figure 1.**  $G$  vs  $z$  traces recorded during break-junction experiments in the presence of OPE-diamine in logarithmic (a) and linear (b) scale. The horizontal dashed lines indicate the  $G$  limits which define the maximum stretching lengths before rupture of OPE-diamine molecular junctions. In part (b), it is easy to see that the fluctuations of the one-plateau traces (two green traces in the middle) are several times the conductance at which the plateaus develop in the broken-plateau traces (last three blue traces at the right).

presence of the OPE-diamine. Plateaus at  $G_0 = 2e^2/h$  ( $e$  being the electron charge, and  $h$  the Planck's constant) of a few tenths of a nanometer form due to the one-atom contact withstanding the stretching.<sup>30</sup> The first 2 traces on the left correspond to clean gold breakages, with no molecular junction formation. After the  $1 G_0$  plateau, there is an abrupt jump in  $G$  due to the sudden opening of a gap between the electrodes, as the elastic strain on the contact is released in the rupture and the gold apex atoms reorganize. After that,  $G$  decays exponentially with  $z$ , indicating that only background

tunneling current is flowing between the electrodes. The rest of traces in Figure 1 display new conductance plateaus around  $10^{-4} G_0$ , which indicate the formation of molecular junctions with one or a few OPE-diamine molecules spanning the electrodes. Similarly as in the case of the gold contacts, these plateaus remain so long as molecular junctions withstand the interelectrode separation without breaking.

We carried out break-junction experiments using a home-built STM operated in ambient conditions.<sup>31</sup> We used commercial gold substrates on quartz (Arrandee), which were cleaned in boiling ethanol and then flame-annealed with a butane flame. As STM tips, we used a 0.25 mm gold wire (99.99%), heated with a butane flame and freshly cut immediately before use. During the break-junction experiment, the tip is moved vertically in and out of contact with the substrate to form and break gold contacts, while the conductance  $G = I/V$  of the circuit is measured. A bias voltage  $V$  of 180 mV was applied between the tip and the substrate, and a linear current-to-voltage converter with two amplification stages was used to measure the current  $I$  in the circuit.

The OPE-diamine used in this work was synthesized following a procedure reported in the literature.<sup>10</sup> The molecules were deposited on the substrate by a drop casting method. Over a freshly clean gold substrate, we deposited a few drops of 1 mM solution of the molecule in 1,2,4-trichlorobenzene (TCB) until the entire sample was covered with solution. We waited 30 min to ensure a high coverage and homogeneous adsorption of the molecules on the substrate. Finally we evaporated the solvent under a nitrogen flow. All the measurements presented in this work were done on the as dried samples, under ambient conditions.

We characterized the response time of our device in order to establish the range of stretching speeds that we can reliably employ. This is determined by the electronic response time as well as for the response time of our STM, in particular, that of the piezo element which controls the tip position. Plateaus indicating the formation of OPE-diamine molecular junctions appear between  $10^{-4}$  and  $10^{-5} G_0$ . In this region, we studied the variation of the slope in the tunneling regime with the speed when performing approach–retract cycles without making contact between the substrate and the tip of the STM. We observed that the tunneling slope stays constant up to 200 nm/s and starts to decrease above this speed (see Figures S1 and S2), and 200 nm/s is then the maximum speed at which our measurements are reliable. On the other hand, the lowest speed limit is given by the drift of our STM. After the microscope has had time to stabilize (around 1 h), we determined the in-plane XY-drift to be  $11 \pm 8$  pm/s. We have explored in our experiments stretching speeds between  $10^2$  and  $10^{-2}$  nm/s.

In our experiments, the resolution in the vertical motion was  $\delta z_{\min} = 1$  pm, and the minimum dwell time was  $\delta t_{\min} = 26 \mu\text{s}$ . For measurements at speeds faster than 40 nm/s, we kept the dwell time to  $\delta t_{\min}$  and used corresponding larger  $\delta z$  values, while for slower speeds, we kept  $\delta z = \delta z_{\min}$  and used corresponding longer dwell times. In all cases, the measurement of the current was always taken only at the end of the dwell time.

## RESULTS AND DISCUSSION

**Single and Multiple Molecular Junctions.** Figure 2a shows the 2D histogram of a set of consecutively measured  $G$  vs  $z$  traces as those shown in Figure 1. The histogram was built after aligning all the traces on the  $z$ -axis just after the breaking of the gold contact ( $z = 0$ ) and using bin sizes of  $\Delta \log(G/G_0) = 0.03$  and  $\Delta z = 0.3$  nm. A clear prominence between  $\log(G/G_0) = -5$  and  $-4$  indicates the preferred conductance and stretching lengths of the plateaus present in individual  $G$  vs  $z$  traces as those of Figure 1. From a visual inspection of the traces displaying plateaus in Figure 1 (last five traces), we can distinguish traces with two kinds of profile. The first group are those traces with one plateau, for which the conductance decreases in a monotonic fashion along the trace (the third and fourth traces in Figure 1, green). We call these ‘one-plateau traces’. The second kind are those traces for which one or

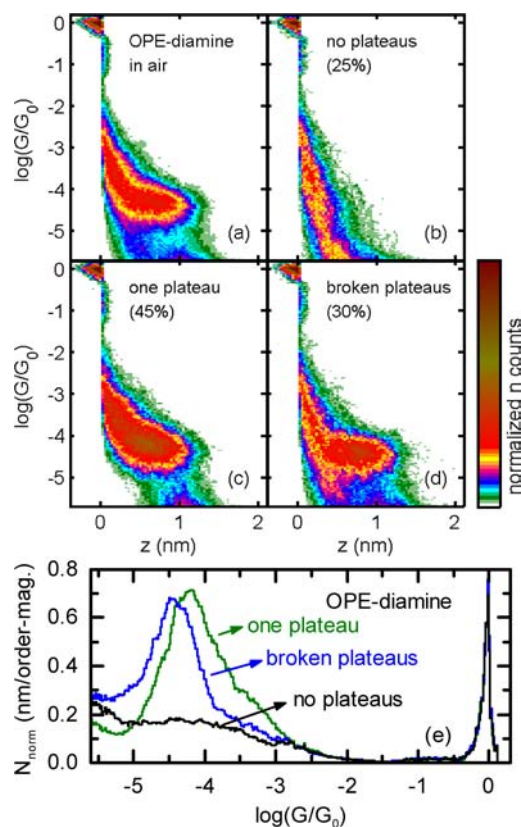


**Figure 2.** (a–d) 2D histograms of a set of 2500 traces consecutively measured at 15 nm/s: (a) all measured traces and (b–d) the same traces divided in traces with no, one, and broken plateaus. The values in brackets correspond to the approximate percentage of traces in each group. (e) 1D histograms for the same traces included in (b–d). The histograms are normalized as previously reported.<sup>19</sup>

several plateaus appear abruptly after the conductance has dropped below  $10^{-5} G_0$ , the lower end of the prominence of the histogram of Figure 2a (last three traces in Figure 1, blue). As this is the lowest conductance at which plateaus are observed, no molecule would be spanning the electrodes during the breakages. We, therefore, call these traces ‘broken-plateau traces’. The abrupt beginning of the plateaus in broken-plateau traces suggests that these can be most frequently due to just one molecule which promptly becomes bound between the electrodes forming a single-molecule junction. In order to explore this possibility, we have separated our traces into groups and analyzed their behavior separately. For each trace, we obtained all the  $z$  values at which the conductance crosses  $10^{-5} G_0$ . We considered that a new plateau forms in the trace and is not just a conductance fluctuation, if there is a  $\Delta z > 0.025$  nm below  $10^{-5} G_0$ , followed by a  $\Delta z > 0.1$  nm above  $10^{-5} G_0$ . The traces verifying this condition constitute the group of broken-plateau traces. From the remaining traces, we separated those with one plateau from those with no plateaus, as those for which an elongation  $\Delta z > 0.1$  nm is needed to produce a decay in conductance of  $\Delta \log(G/G_0) = 0.1$  at any region below  $0.5 G_0$ .<sup>19,31</sup>

In Figure 2b–d, we show the 2D histograms of the traces with no, one, or broken plateaus, while the corresponding 1D log  $G$  histograms are shown in Figure 2e. First, we see that the initial tunneling region at the left of 0.5 nm shows a smoother transition to the plateau prominence for one-plateau traces (Figure 2c) than for broken-plateau ones (Figure 2d),

suggesting that the molecular junctions are formed at short gap sizes (or even before the gold contact is broken) for the former, while no molecular junction is yet formed in the case of the latter. In addition, the plateau prominence or peak is centered at lower  $G$  values for broken-plateau traces. This is consistent with the picture that, on average, a lower number of molecules (or even just one) take part in these junctions, when they finally form.

One potential explanation of the one-plateau traces could be that they correspond to single-molecule junctions with a different more stable conformation than for the broken-plateau cases. The length of the prominences on the 2D histograms of one-plateau traces shows that their plateaus can last for around 1 nm without breaking. Theoretical calculations estimate the elastic stretching of single-molecule junctions based in different diamine compounds in values between 0.1 and 0.16 nm (measured from the relaxed geometry until reaching the maximum tensile force).<sup>15,18,28,29</sup> It is then difficult to explain how a single molecule would be able to generate plateaus 1 nm long without breaking. Alternatively, one-plateau traces can be due to junctions with several molecules taking part and helping to stabilize it. Indeed, the conductance fluctuations of the one-plateau traces shown in Figure 1b are compatible with the attachment and detachment of individual molecules in a junction with several of them taking part. While the electrodes are separated, some of several molecules in the junction can detach while new ones attach in gold sites closer to the electrode apex, so that the plateau persist without breaking below  $10^{-5} G_0$ . In the next section we will discuss in detail the behavior under stretching of the junctions, which provides extra information to support this idea.

**Dependence of the Junction Behavior with the Stretching Speed.** We now study separately the behavior for one- and broken-plateau traces as the stretching speed of the break-junction cycles is varied. During our experiments, we observed that the percentage of traces displaying no, one, or broken plateaus remains practically constant with the speed, with average values of 25%, 45%, and 30% respectively, with approximately a 10% uncertainty (Figure S3).

We obtained the typical conductance for each group by fitting a Gaussian to the overall peaks of the 1D histograms as in Figure 2e. The conductance values are the maxima of the corresponding log-normal distributions in the linear scale:<sup>32</sup>  $G_{\text{broken}} = 2.6 \pm 1.6 \times 10^{-5} G_0$  and  $G_{\text{one}} = 3.6 \pm 1.6 \times 10^{-5} G_0$  (Figures S4 and S5). The conductance values of both sets of traces are similar because one-plateau traces frequently stabilize at a conductance value close to that of broken-plateau traces, specially at the end of the trace. This is reflected in a high probability of this value in the linear histogram. This is easy to understand in the picture of these traces being due to junctions with several molecules, as it seems reasonable that they tend to terminate ultimately with just a single molecule in the junction before they finally break. We observe that for both one- and broken-plateau traces, the conductance stays practically constant with the speed. There is a slight increase in the average junction conductance as the speed is decreased, which is due to a higher weight of conductance values larger the single-molecule one (Figures S4 and S5). This suggests that, when moving the electrodes more slowly, it becomes more probable that extra molecules join the junctions along the stretching. We see that our criterion for separating the traces is not pure. As mentioned, junctions with multiple molecules can still have an important contribution of single-molecule



conductance values. Correspondingly, broken-plateau traces can also contain contributions from multiple-molecule junctions that form before the first breakage, and we will expect too that after a single-molecule junction is formed, other molecules can join afterward.

Regarding the molecular junction elongation, we have analyzed one- and broken-plateau traces in different ways. For broken-plateau traces, the abrupt beginning and end of the plateaus indicate the intermittent formation and rupture of the molecular junctions. We measure their individual stretching length  $L_s$  as the  $z$  interval between two consecutive up-down crosses of the trace at  $10^{-5} G_0$ , verifying the same conditions mentioned before (a  $\Delta z > 0.025$  nm below  $10^{-5} G_0$ , followed by a  $\Delta z > 0.1$  nm above  $10^{-5} G_0$ ). This definition is illustrated in Figure 1.

The probability that an individual molecular junction breaks after a given stretching  $L_s$  is then obtained as  $P_{\text{break}}(L_s) = N(L_s)/N_{\text{tot}}$ , with  $N(L_s)$  being the number of plateaus with length  $L_s$  and  $N_{\text{tot}}$  being the total number of considered plateaus. Figure 3a shows that this probability decays

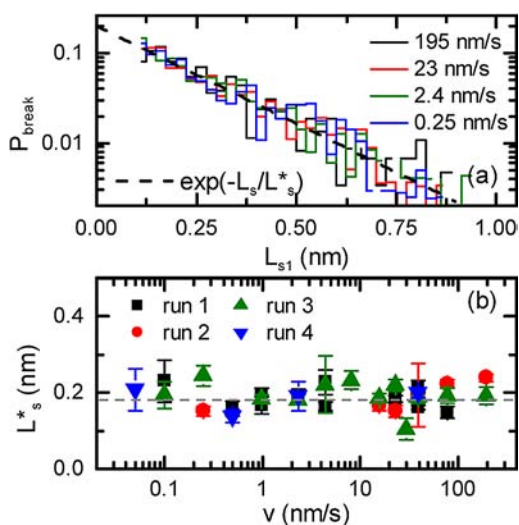


**Figure 3.** (a) Distributions of the length of individual plateaus  $L_s$  at different stretching rates, obtained from broken-plateau traces. The dashed line correspond to the fit of  $P \propto \exp(-L/L_s^*)$  to our data. (b) Values of  $L_s^*$  obtained at different stretching rates for four different experimental runs.

exponentially with the length. The figure also shows that the probability distribution stays rather constant when varying the stretching speed over 3 orders of magnitude. Figure 3b shows the values of the characteristic length  $L_s^*$ , obtained by fitting the expression  $P_{\text{break}} \propto \exp(-L_s/L_s^*)$  to distributions as those of Figure 3a obtained over four different experimental runs.  $L_s^*$  stays practically constant at  $0.18 \pm 0.1$  nm. This value is quite close to that mentioned above, estimated by theoretical calculations for the elastic stretching of a junction held by two amine–gold bonds.<sup>15,18,28,29</sup> In other words, these junctions can be stretched, on average, as much as that predicted for a single-molecule junction, supporting our hypothesis of the previous section. As a consequence of  $L_s^*$  being constant, the characteristic time span of the junction  $L_s^*/v$  increases while  $v$  decreases, reaching around 2 s at the slowest tested speed.

Over the studied range of stretching speeds, the rupture of molecular junctions has been previously related to the thermal

breakdown of the chemical bond under an applied tensile force.<sup>21,24,33</sup> For first-order thermal desorption processes, the rate of desorption of  $N_a$  molecules adsorbed to a surface is described by the expression<sup>34</sup>  $dN_a(t)/dt = -N_a(t)/\tau$ . Here,  $\tau$  is the lifetime of the adsorbed state (or residence time) and is given by the Arrhenius equation:  $\tau = \tau_0 \exp(E_b/k_B T)$ , where  $E_b$  is the binding energy,  $k_B$  is the Boltzmann constant, and  $T$  is the temperature. In our measurements, we move at a constant speed, so that time and elongation are proportional ( $L_s = v\Delta t$ ). Assuming that the adsorption lifetime  $\tau$  is unaffected by tensile forces in the expression for the desorption rate, we could expect  $P_{\text{break}}(L_s) \propto \exp(-L_s/v\tau)$ , if the junction breakage would be caused by spontaneous molecule desorption. Figure 3a shows that  $P_{\text{break}}$  does follow such an exponential decay. However, this expression would lead to  $L_s^* = v\tau$ , and in contrast, our decay length  $L_s^*$  stays constant with  $v$ . Note that if  $\tau$  would depend on the applied tensile force, the predicted expression for  $P_{\text{break}}(L_s)$  due to desorption would not be an exponential, but it would still depend on the stretching speed.<sup>35</sup> We conclude therefore that the observed probability distributions of Figure 3a do not reflect the stochastic desorption of the molecules from the electrodes and that the absorption lifetime  $\tau$  in our case must be much larger than the characteristic time span observed at any speed. In particular,  $\tau$  must be  $>2$  s. Using a typical value for the vibrational lifetime  $\tau_0 = 10^{-13}$  s in the above expression for  $\tau$ ,<sup>34,36</sup> this means  $E_b/k_B T > 30$ , which is compatible with values of the binding energies  $E_b$  for diamines on gold of around 1–0.8 eV reported in the literature for 1,4-diaminobenzene.<sup>15</sup> Specifically, we deduce that the absorption lifetime is, at least, 10 times larger than that previously reported for 1,4-diaminobenzene.<sup>24</sup> In that work, along the same range of stretching speeds studied here, the junction rupture is described to change from a force-accelerated spontaneous breaking to a self-breaking regime. In contrast, our results indicate that the OPE-diamine junctions stay in the force-break regime (using the authors nomenclature).<sup>23,24</sup> The lack of speed dependence in our measurements also suggest that there is no significant local heating along our measurements, in contrast with that previously proposed for alkane dithiols.<sup>22</sup> The distributions of stretching length of Figure 3a are most likely determined by the geometrical positioning of the individual molecules between the electrodes. Indeed, the amine–gold bond takes place through the  $sp^3$  hybridized lone pair of N, which forms directional dative bonds to gold, and, hence will be sensitive to the detailed orientation of the anchoring group with respect to the gold atoms, which will change when stretching the junction.

We next studied the maximum electrode displacement before rupture for one-plateau traces. In this case, we define the total displacement length  $L_t$  as the  $z$  interval that the conductance takes to decay from 0.5 to  $10^{-5} G_0$  (illustrated in Figure 1). Figure 4a shows the probability distributions of the junctions to break at a given  $L_t$  at different speeds for one-plateau traces. Figure 5a shows the mean value of these distributions  $L_t^*$  versus the speed, for four different experimental runs, obtained by fitting a Gaussian to the distributions like those of Figure 4a. The error bars in Figure 5 correspond to the standard deviation (width) of the distributions. We observe that again  $L_t^*$  stays practically constant along the whole range of studied speeds, indicating once more that the molecular-junction breakage is not due to the thermal desorption of the molecules at any explored speed. The characteristic time span  $L_t^*/v$  reaches now  $\sim 10$  s at the slowest speed, which shows the high stability that

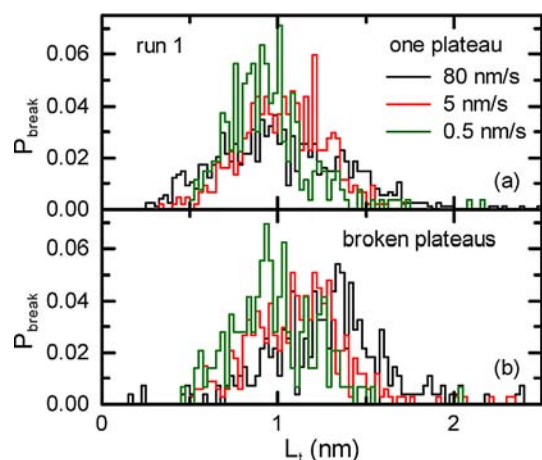


**Figure 4.** Distributions of probability that an OPE-diamine junction breaks after a total stretching distance  $L_t$  for different stretching rates, obtained from traces with one (a) and broken (b) plateaus.

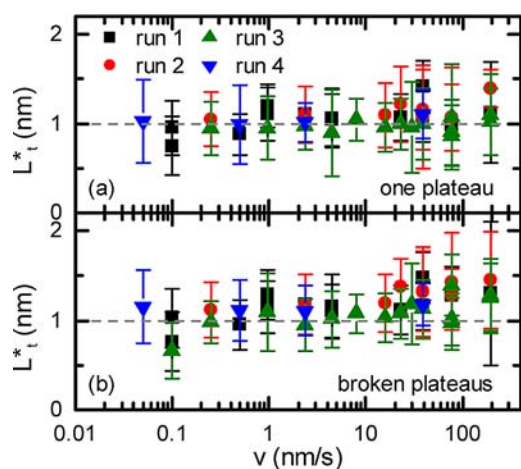


**Figure 5.** Mean value of the probability distributions as those of Figure 4 as a function of the stretching rate  $\nu$  for traces with one (a) and broken (b) plateaus. The different symbols correspond to data from different experimental runs, and the error bars are given by the width of the distributions. The dashed lines at 1 nm are guides for the eye.

can be obtained for molecular junctions with amine anchor groups. This time interval is significantly larger than the 2 s obtained for individual broken plateaus. This result is easy to understand assuming that one-plateau traces are due to junctions with several attached molecules. Along these plateaus, some of the molecules are probably detaching, while new ones are attaching closer to the electrode apex, so that there is always at least one molecule holding the junction together. As mentioned in the previous section, the conductance fluctuations along the traces are compatible with this model (see Figure 1). The elongation limit would now not be the stretching of an individual gold–amine bond but simply corresponds to an interelectrode distance smaller than, or equal to, the length of the molecule. The length of the studied OPE-diamine is 2.1 nm.<sup>37</sup> Accounting for a typical retraction of the electrode apices of 0.4 nm,<sup>19</sup> we would expect maximum  $L_t$  values around 1.7 nm. This value agrees well with the  $L_t$  values at the right-end of the distributions as those of Figure 4a (shown in Figure S6), as previously reported for alkane-diamines.<sup>19</sup>

As just described, the different behavior upon stretching of broken- and one-plateau traces can be consistently explained by introducing the idea that broken plateaus are most frequently due to single-molecule junctions, while one plateaus are due to junctions with several molecules. We cannot completely exclude the possibility that the two kinds of plateaus are due to two different junction configurations. However, as already mentioned, this picture is more difficult to reconcile with our observations. In particular, it is difficult to explain how a single molecule would be able to generate plateaus 1 nm long. It has been suggested that a molecule could slide along the electrode surface until reaching the apex, jumping between neighboring gold sites.<sup>18,38</sup> However, considering that an amine–gold bond is expected to stretch <0.2 nm, this will mean that the molecule will have to slide along 5 or 6 gold sites without an abrupt breakage. Looking at the distribution of Figure 4a for broken-plateau traces, the probability of having plateaus with a length close to 1 nm is extremely low. It is then difficult to explain how a different type of single-molecule junction will be able to generate another 45% of the traces that reach this length without any breakage.

Finally, although for broken-plateau traces junctions form and break before reaching  $L_t$ , we show their corresponding  $L_t$  distributions in Figure 4b for comparison with those for one-plateau traces. The resulting  $L_t^*$  is shown in Figure 5b. We observe that the  $L_t^*$  values for broken-plateau traces are slightly higher than for one-plateau traces. There is also an increase of  $L_t^*$  for stretching speeds over 20 nm/s, which is concurrent with a larger dispersion value (larger error bars). The dispersion also increases in this range for one-plateau traces (see also Figure S7 for the variation of the  $L_t$  values at the right end of the distributions with  $\nu$ ) but to a lesser extent.

Different reports in the literature show a dependence of the molecular junction length with speed for alkane dithiols<sup>21,22</sup> and benzene dithiols/diamines,<sup>24,33</sup> over a similar range of stretching speeds. The observed length variations were <0.2 nm, but this constitutes an important length change for these short molecules. In our case, we observed measurement-to-measurement variations of  $L_t$  at a fixed speed which is >0.2 nm (see Figure 5). A similar variation to that shown in Figure 5b has also been reported for an OPE-dithiol.<sup>39</sup> However, in our case, we only observed some variation with the stretching speed for  $L_t$  in broken-plateau traces, for which we have strong evidence that  $L_t$  is not the stretching before rupture of a single molecule between the electrodes but just the maximum electrode displacement at which we observe a junction signature. This indicates that this variation is not due to a change in the molecule–electrode bond breakage process but most probably to variations in the behavior of the gold. It is well-known that after a gold contact is broken, the electrodes suffer a fast retraction due to atomic relaxation at their apices. When moving slowly enough, this retraction can completely take place between two consecutive measured points, producing a sharp jump in conductance just below 1  $G_0$ . However, when the pulling speed is increased, we can force the separation of the electrodes before the atomic relaxation is finished, so that the  $G$  vs  $z$  traces would be recorded with a smaller electrode retraction than at slower pulling speeds, and we thus would expect a larger apparent total stretching length, as we observed for  $L_t$  in Figure 5b. Indeed, we have evidence that this is the case in some experimental runs (see Figures S7 and S8). For speeds above  $\sim 10$  nm/s, we observed a decrease in the initial gold electrode retraction which indicates that the

gold atoms do not have time to fully relax before we start separating our electrodes. We observe differences in the behavior along different experimental runs, reflecting the fact that the relaxation process will depend on the geometric and environmental details of each particular electrode. How far the tip crashes into the surface will also influence the gold electrode retraction. However we have observed that this influence is no larger than the uncontrollable electrode details: We observe a clear correlation between the crashing depth and the subsequent electrode retraction in some experiments, while there is no observable correlation in others.

The different behavior between the  $L_t^*$  for one- and broken-plateau traces is also consistent with our previous hypothesis about the origin of both kinds of trace. If one-plateau traces are due to molecular junctions that form before (or at an early stage after) the gold breakage, the binding points to the electrodes are expected to be, on average, at a greater distance from the electrode apex than those formed once the gap is well opened. Accordingly, they will, on average, break at shorter gap sizes (shorter  $L_t$  values) and will also be less sensitive to the electrode apex relaxation. This is reflected in values of  $L_t^*$  for one-plateau traces which are lower and less stretching rate dependent than those for broken-plateau traces.

## CONCLUSIONS

In summary, using a scanning tunneling microscope, we have studied the elongation of molecular junctions of OPE-diamine as a function of the stretching rate under ambient conditions. We found that the high directional character of the amine–gold bond leads to ruptures along the pulling traces, which allows us to disentangle the evolution details of the junctions and differentiate between junctions formed most probably by one and those probably formed by several molecules. For ~30% of the stretching processes, we observe the signature of junctions most likely containing just one molecule, which have a mean conductance of  $2.6 \pm 1.6 \times 10^{-5} G_0$ . In these cases, more than one molecular junction can fully break and reform along an individual pulling event. For another 45% of the experiments, junctions seem to be formed by several molecules. These junctions last until the interdistance between the electrode tips becomes larger than the molecule size, with individual participating molecules probably detaching and attaching along the pulling trace. In both cases, the stretching length of the OPE-diamine molecular junctions remains constant in the studied range of stretching speeds (0.1–100 nm/s). We hence observe no indication of thermally induced desorption in our measurements. The adsorption lifetime of the amine–gold bond should therefore be much larger than 2 s, and the junction breakage should primarily be caused by the growth of the gap between the gold electrodes and the elastic limit of amine–gold bonds.

## ASSOCIATED CONTENT

### Supporting Information

Study of the response time of the experimental setup; percentage, conductance, and maximum total displacement length before rupture of one- and broken-plateau traces for different stretching speeds; examples of conductance histograms in the linear scale; 2D histograms of  $G$  vs  $z$  traces; and estimation of the initial interelectrode gap size obtained at different stretching speeds. This material is available free of charge via the Internet at <http://pubs.acs.org>.

## AUTHOR INFORMATION

### Corresponding Author

teresa.gonzalez@imdea.org

### Notes

The authors declare no competing financial interest.

## ACKNOWLEDGMENTS

This work was supported by the Spanish Ministerio de Economía y Competitividad through the projects MAT2011-25946, RYC-2008-03328, and CSD2007-0010 (Consolidación-ingeniería, nanociencia molecular), the CAM through the project S2009/MAT-1726 (Nanobiomagnet), and the EU through the network FUNMOLS (grant no. PITN-GA-2008-212942). E.L. was funded through the EU by the ELFOS network (FP7-ICT2009-6).

## REFERENCES

- (1) Xu, B.; Tao, N. *Science* **2003**, *301*, 1221–1223.
- (2) Chen, F.; Li, X.; Hihath, J.; Huang, Z.; Tao, N. *J. Am. Chem. Soc.* **2006**, *128*, 15874–15881.
- (3) Venkataraman, L.; Klare, J. E.; Tam, I. W.; Nuckolls, C.; Hybertsen, M. S.; Steigerwald, M. L. *Nano Lett.* **2006**, *6*, 458–462.
- (4) Li, Z.; Pobelov, I.; Han, B.; Wandlowski, T.; Blaszczyk, A.; Mayor, M. *Nanotechnology* **2007**, *18*, 044018.
- (5) Wu, S.; Gonzalez, M. T.; Huber, R.; Grunder, S.; Mayor, M.; Schoenenberger, C.; Calame, M. *Nat. Nanotechnol.* **2008**, *3*, 569–574.
- (6) Fock, J.; Sorensen, J. K.; Lortscher, E.; Vosch, T.; Martin, C. A.; Riel, H.; Kilsa, K.; Bjornholm, T.; van der Zant, H. *Phys. Chem. Chem. Phys.* **2011**, *13*, 14325–14332.
- (7) Loertscher, E.; Gotsmann, B.; Lee, Y.; Yu, L.; Rettner, C.; Riel, H. *ACS Nano* **2012**, *6*, 4931–4939.
- (8) Venkataraman, L.; Klare, J. E.; Nuckolls, C.; Hybertsen, M. S.; Steigerwald, M. L. *Nature* **2006**, *442*, 904–907.
- (9) Mishchenko, A.; Vonlanthen, D.; Meded, V.; Burkle, M.; Li, C.; Pobelov, I. V.; Bagrets, A.; Viljas, J. K.; Pauly, F.; Evers, F.; Mayor, M.; Wandlowski, T. *Nano Lett.* **2010**, *10*, 156–163.
- (10) Lu, Q.; Liu, K.; Zhang, H.; Du, Z.; Wang, X.; Wang, F. *ACS Nano* **2009**, *3*, 3861–3868.
- (11) Wang, C.; Batsanov, A. S.; Bryce, M. R.; Martin, S.; Nichols, R. J.; Higgins, S. J.; Garcia-Suarez, V. M.; Lambert, C. J. *J. Am. Chem. Soc.* **2009**, *131*, 15647–15654.
- (12) Reddy, P.; Jang, S.-Y.; Segalman, R. A.; Majumdar, A. *Science* **2007**, *315*, 1568–1571.
- (13) Malen, J. A.; Yee, S. K.; Majumdar, A.; Segalman, R. A. *Chem. Phys. Lett.* **2010**, *491*, 109–122.
- (14) Loertscher, E.; Cizek, J. W.; Tour, J.; Riel, H. *Small* **2006**, *2*, 973–977.
- (15) Frei, M.; Aradhya, S. V.; Koentopp, M.; Hybertsen, M. S.; Venkataraman, L. *Nano Lett.* **2011**, *11*, 1518–1523.
- (16) Frei, M.; Aradhya, S. V.; Hybertsen, M. S.; Venkataraman, L. *J. Am. Chem. Soc.* **2012**, *134*, 4003–4006.
- (17) Nef, C.; Frederix, P. L. T. M.; Brunner, J.; Schoenenberger, C.; Calame, M. *Nanotechnology* **2012**, *23*, 365201.
- (18) Kamenetska, M.; koentopp, M.; Whalley, A. C.; Park, Y. S.; Steigerwald, M. L.; Nuckolls, C.; Hybertsen, M. S.; Venkataraman, L. *Phys. Rev. Lett.* **2009**, *102*, 126803.
- (19) Arroyo, C. R.; Leary, E.; Castellanos-Gomez, A.; Rubio-Bollinger, G.; Gonzalez, M. T.; Agrait, N. *J. Am. Chem. Soc.* **2011**, *133*, 14313–14319.
- (20) Franco, I.; Solomon, G. C.; Schatz, G. C.; Ratner, M. A. *J. Am. Chem. Soc.* **2011**, *133*, 15714–15720.
- (21) Huang, Z.; Chen, F.; Bennett, P. A.; Tao, N. *J. Am. Chem. Soc.* **2007**, *129*, 13225–13231.
- (22) Huang, Z.; Chen, F.; D'Agosta, R.; Bennett, P. A.; Di Ventra, M.; Tao, N. *Nat. Nanotechnol.* **2007**, *2*, 698–703.
- (23) Tsutsui, M.; Shoji, K.; Taniguchi, M.; Kawai, T. *Nano Lett.* **2008**, *8*, 345–349.



- (24) Tsutsui, M.; Taniguchi, M.; Kawai, T. *J. Am. Chem. Soc.* **2009**, *131*, 10552–10556.
- (25) Haiss, W.; Nichols, R.; van Zalinge, H.; Higgins, S.; Bethell, D.; Schiffrin, D. *Phys. Chem. Chem. Phys.* **2004**, *6*, 4330–4337.
- (26) Li, C.; Pobelov, I.; Wandlowski, T.; Bagrets, A.; Arnold, A.; Evers, F. *J. Am. Chem. Soc.* **2008**, *130*, 318–326.
- (27) Gonzalez, M. T.; Brunner, J.; Huber, R.; Wu, S.; Schoenenberger, C.; Calame, M. *New J. Phys.* **2008**, *10*, 065018.
- (28) Zotti, L. A.; Kirchner, T.; Cuevas, J.-C.; Pauly, F.; Huhn, T.; Scheer, E.; Erbe, A. *Small* **2010**, *6*, 1529–1535.
- (29) Kim, Y.; Hellmuth, T. J.; Buerkle, M.; Pauly, F.; Scheer, E. *ACS Nano* **2011**, *5*, 4104–4111.
- (30) Agrait, N.; Yeyati, A.; van Ruitenbeek, J. *Phys. Rep.* **2003**, *377*, 81–279.
- (31) Gonzalez, M. T.; Leary, E.; Garcia, R.; Verma, P.; Herranz, M. A.; Rubio-Bollinger, G.; Martin, N.; Agrait, N. *J. Phys. Chem. C* **2011**, *115*, 17973–17978.
- (32) Huber, R.; Gonzalez, M. T.; Wu, S.; Langer, M.; Grunder, S.; Horhoiu, V.; Mayor, M.; Bryce, M. R.; Wang, C.; Jitchati, R.; Schoenenberger, C.; Calame, M. *J. Am. Chem. Soc.* **2008**, *130*, 1080–1084.
- (33) Tsutsui, M.; Shoji, K.; Morimoto, K.; Taniguchi, M.; Kawai, T. *App. Phys. Lett.* **2008**, *92*, 223110.
- (34) Thomas, J. M.; Thomas, W. J. *Principles and Practice of Heterogeneous Catalysis*; Wiley-VCH Verlag: Weinheim, Germany, 1997.
- (35) Evans, E. *Faraday discussions* **1998**, *111*, 1–16.
- (36) Attard, G.; Barnes, C. *Surfaces*; Oxford University Press: Oxford, U.K., 1998.
- (37) We estimate the molecular length using hyperchem, as the maximum distance between the centers of two gold atoms attached to the nitrogen atoms at the extremes of the molecule. The gold–nitrogen bonds form an angle of 107° with the backbone of the molecule.
- (38) Paulsson, M.; Krag, C.; Frederiksen, T.; Brandbyge, M. *Nano Lett.* **2009**, *9*, 117–121.
- (39) Kaliginedi, V.; Moreno-Garcia, P.; Valkenier, H.; Hong, W.; Garcia-Suarez, V. M.; Buitter, P.; Otten, J. L. H.; Hummelen, J. C.; Lambert, C. J.; Wandlowski, T. *J. Am. Chem. Soc.* **2012**, *134*, 5262–5275.